

Thermo-physical evaluation of hybrid-nanofluids zeotropic mixtures in a vapor compression refrigeration system

Buhar sıkıştırılmalı soğutma sistemindeki hibrit-nanoakışkan zeotropik karışımların termo-fiziksel değerlendirilmesi

Akanimo Ekpenyong Udofia¹ , Aniekan Essienubong Ikpe*² 

¹Department of Aerospace Engineering, Federal University of Science and Technology, Ikot Abasi, Nigeria.

²Department of Mechanical Engineering, Akwa Ibom State Polytechnics, Ikot Osurua, PMB 1200, Nigeria.

• Received: 26.12.2022

• Accepted: 19.08.2024

Abstract

This research involves an experimental study of vapour compression refrigeration system (VCRS) with hybrid-nanofluids zeotropic blends of (23%-R32/25%-R125/52%-R134a) in the ratio of (0.03 - 0.15 % Vol.) with elven samples as thus: 001, 010, 100, 011, 111, 211, 121, 112, 221, 212 and 122 gram). A morphology characterization test was conducted using scanning electron microscope (SEM) and X-ray Diffraction (XRD) amongst the selected ratios using compressor work efficiency, power consumption rate and Coefficient of performance (COP) as the core enhancement parameters. The most favorable blend produced the optimum COP in three different fraction ratios (011, 111 and 112). The outcome indicated that thermo-physical and vapor compression properties of hybrid-nanofluids zeotropic (011) zero gram-TiO₂, 7.5g-Al₂O₃/CuO; (112) 3.75 g-TiO₂/Al₂O₃, 7.5 g-/CuO and (111) 5.0g-TiO₂/Al₂O₃/CuO produced the best optimum performance of 3.1%, 1.41% and 1.21% respectively. The COP was found to be highest at (011) blend by about 3.1% at refrigerant temperature of -7 °C. The maximum compressor power coefficient, volumetric cooling capacity and TEGWI were found to increase by 13.51%, 5.78 % and 1.06 kg/sec CO₂. The study also revealed that nanoparticles mixed in the base fluid increased the heat transfer coefficient even with a smaller particle portion of 0.003%, with optimum improvement of 0.0075 Vol % application. The calculated values of exergy destruction in each component at various % fractions are presented in Appendix I. Outcome of the study confirmed that hybrid-nanofluids zeotropic blend is energy efficient and environmentally friendly with good characteristics healthier than CFCs and HCFCs, and can offer healthier compressor/refrigerator working fluid substitute to be adopted in VCRS and air conditioning operations.

Keywords: Coefficient of performance, Eco-friendly, Hybrid-nanofluids, Refrigerants, Refrigeration system.

Öz

Bu araştırma, (0.03 - 0.15 % Vol.) oranında (%23-R32/%25-R125/%52-R134a) hibrit-nanoakışkan zeotropik karışımlara sahip buhar sıkıştırılmalı soğutma sisteminin (VCRS) deneysel bir çalışmasını içermektedir. Vol.) elf numuneleri şu şekildedir: 001, 010, 100, 011, 111, 211, 121, 112, 221, 212 ve 122 gram). Temel geliştirme parametreleri olarak kompresör iş verimliliği, güç tüketim oranı ve performans katsayısı (COP) kullanılarak seçilen oranlar arasında taramalı elektron mikroskopu (SEM) ve X-ışını kırınımı (XRD) kullanılarak bir morfoloji karakterizasyon testi gerçekleştirildi. En uygun karışım, üç farklı fraksiyon oranında (011, 111 ve 112) optimum COP'yi üretti. Sonuç, hibrit nanoakışkanların zeotropik (011) sıfır gram-TiO₂, 7.5g-Al₂O₃/CuO; (112) 3,75 g-TiO₂/Al₂O₃, 7,5 g-/CuO ve (111) 5,0g-TiO₂/Al₂O₃/CuO sırasıyla %3,1, %1,41 ve %1,21 ile en iyi optimum performansı üretti. COP'nin (011) karışımında -7 oC soğutucu akışkan sıcaklığında yaklaşık %3,1 oranında en yüksek olduğu bulunmuştur. Maksimum kompresör güç katsayısının, hacimsel soğutma kapasitesinin ve TEGWI'nin sırasıyla %13,51, %5,78 ve 1,06 kg/sn CO₂ oranında arttığı bulunmuştur. Çalışma aynı zamanda baz akışkana karıştırılan nanopartiküllerin %0,003'lük daha küçük bir partikül kısmı ile bile ısı transfer katsayısını artırdığını ve %0,0075 Hacimlik optimum uygulama iyileştirmesini ortaya çıkardı. Her bir bileşendeki ekserji yıkımının çeşitli % oranlarında hesaplanan değerleri Ek I'de sunulmaktadır. Çalışmanın sonucu, hibrit-nanoakışkan zeotropik karışımın enerji açısından verimli ve çevre dostu olduğunu, CFC'ler ve HCFC'lerden daha sağlıklı iyi özelliklere sahip olduğunu ve daha sağlıklı kompresör sunabileceğini doğruladı. /buzdolabı çalışma sıvısı ikamesi, VCRS ve iklimlendirme operasyonlarında kullanılacaktır.

Anahtar kelimeler: Performans katsayısı, Çevre dostu, Hibrit nanoakışkanlar, Soğutucular, Soğutma sistemi

*Aniekan Ikpe; aniekan.ikpe@akwaibompoly.edu.ng

1. Introduction

With the advent of electric motors and consequently higher speeds compressors, the scope of applications of refrigeration became widened. The first development took place in 1834 when Perkins proposed a hand-operated compressor machine working on ether. The pace of development was considerably quickened in the 1920 decade when du Pont introduced some new working refrigerants in the market, such as fluoro-chloro derivatives of methane, ethane-popularly known as chloro fluorocarbon CFCs, under the name “Feron” (Imre et al., 2019). To address the present energy crisis and the damaging ecological effect of these refrigerants, and as well improve the performance coefficient and power consumption of the system, several avenues to substitute energy have been investigated. Such growth has developed to embrace Nano lubricants and nanorefrigerants which enhances the working efficiency of refrigeration or thermal systems. These Nanolubricant, simply known as nanofluids, have an outstanding physical characteristics from heat transfer coefficient to physical and mechanical properties. The term “refrigeration” is used to denote maintenance of a system or body at a temperature lower than that of its surroundings. Hence, it is the process of cooling a substance below the initial temperature of the substance. Refrigeration systems have been a subject of continuous modifications and developments in order to meet the specific demand of the fast-growing population in the world.

Refrigeration process functions through a liquid refrigerant which absorbs heat from a low pressure zone (evaporator) by means of its evaporation. This heat is dissipated in a zone of higher pressure (condenser) by means of condensation. The refrigerant absorbs the heat at evaporator through evaporation. The vapour refrigerant is pumped by a compressor which increases the refrigerant pressure to a level where it condenses at normal temperature of the cooling medium (Babarinde et al., 2015). Thus, four fundamental steps which are required to accomplish the above mechanical operation cycle includes: evaporation, compression, condensation and expansion. Once the process take effect, heat is either absorbed or expelled by the system, resulting in a change in temperature of the surrounding air passing over the unit’s components. Nearly all of the refrigeration systems we use today operate through this cycle to accomplish cooling, and the energy consumed by this systems is high globally. The thermodynamic performance, working condition, impact on the environment, and economic feasibility of this systems are greatly determined by characteristics of the working fluid-refrigerant (Imre et al., 2019; Zhang et al., 2017). Hence, selecting a suitable environmentally friendly working fluid-refrigerant becomes one of the major concerns to refrigeration systems. In the early days natural refrigerants such R11, R12, CO₂ and Ammonia which are not very efficient were used, as some of these refrigerants were found to be highly flammable and some extremely toxic. In 1930, scientist’s developed Chlorofluorocarbons (CFCs) that was nonflammable, nontoxic, non-corroded gases and cheap to produced, but shortly it was observed to be an instrument for ozone layer depletion (Baskaran & Mathews, 2012).

Then in the late 70s and early 80s, scientists developed Hydrochlorofluorocarbon (HCFC’s) which had far more damaging effect on the ozone layer because they contained chlorine molecules. Therefore, to clear off this threat, there was advent of Hydrofluorocarbon (HFCs) which do not contain chlorine and was perceived to have negligible or no effect on ozone layer, but however, did not solve the problem since they are greenhouse gases (Krauzina et al., 2017). Afterwards, it was found that the refrigerant is depleting the ozone layer (ODP) and causing global warming potential, hence, these necessitated the need to search for new environmentally friendly refrigerants that possess excellent heat transfer characteristics. In recent times, attention is on using new mixtures that have the same properties as past refrigerants to phase out damaging halogenated substances, in agreement to the Montreal and Kyoto Protocol. Hence, blends of hybrid-nanofluid-zeotropic mixtures have the potential of meeting these requirements (Baskaran & Mathews, 2012; Akanimo et al., 2022). Interestingly, the thermodynamic processes involved in cooling systems release large amount of heat to the environment. Heat transfer between the system and the surrounding environment takes place at a finite temperature difference, which is a major source of irreversibility for the cycle. The losses in the cycle need to be evaluated considering individual thermodynamic process that make up the cycle. The first law is only concerned with the conservation of energy, and it gives no information on how, where, and how much the system performance is degraded. Exergy analysis is a powerful tool in design, optimization and performance evaluation of any energy systems. An exergy analysis is usually aimed to determine the maximum performance of the system and identify the sites of energy destruction.

Meanwhile, [Anand & Tyagi \(2020\)](#) presented theoretical work that involved an extensive review of recent refrigerant mixtures which are being used in refrigeration, air conditioning, and heat pump units. From the study, azeotropic, near azeotropic, and zeotropic mixture properties indicated different properties such as thermodynamic, thermo-physical, chemical, and environmental in different evaporator temperature applications such as domestic, commercial, and automobile systems. [Bhattad et al. \(2018\)](#) reported that the use of Nano particles as working fluids can improve the thermal properties of cooling units (refrigerant) with efficient heat transfer coefficient with its viscosity and thermal conductivity, thereby decreasing the energy intake of the system. Also, some researchers like [Paula de et al. \(2020\)](#) carried out a design on the environmental assessment, energy consumption of a VCR System using R290, R1234yf, and R744 as an alternatives replacement to R134a using exergy investigation for checking the feasibility of hydrocarbons. Results obtained indicated that hydrocarbons are the possible future hope to serve the already depleting environment from the worst case scenario. [Akanimo et al. \(2022\)](#) conducted a study on exergy performance assessment of hybridize-nano-fluids zeotropic blend as refrigerant replacement in VCRS. The findings showed optimum evaporator temperature performance of -7 ($^{\circ}\text{C}$), with power consumption of 0.942 kW and compressor work input of 0.888 (kJ/kg), resulting in efficient thermal conductivity heat transfer performance of 0.962 W/m.K. [König-Haagen et al. \(2019\)](#) conducted an experiment to assess the energy performance of both R404A and R507A refrigerants in a double-stage vapour compression refrigeration system with a sub-cooler heat exchanger in a double-stage vapour compression refrigeration system. The results revealed that R404A has good performance at a high evaporator temperature application and R507A is suitable at low-temperature applications. [Flores et al. \(2019\)](#) presented a theoretical work to analyze the “performance of a cascading system” by using an ozone friendly refrigerant pair. The results pointed out that COP of the system improved from 0.7851 to 1.232 when the evaporator temperature increased from -80 $^{\circ}\text{C}$ to -50 $^{\circ}\text{C}$ with the other parameters kept constant. However, the COP was observed to decrease from 0.9274 to 0.5486 when the condenser temperature increased from 25 $^{\circ}\text{C}$ to 50 $^{\circ}\text{C}$.

[Selvam et al. \(2016\)](#) conducted a research involving silver Nano fluids in an ethylene glycol and water mixture. The thermo-physical parameters such as viscosity, thermal conductivity, density, and specific heat were measured using thermal properties analyzer (KD2 Pro) to determine the outcomes. The thermal conductivity increased as the concentration of Nano particles and the temperature of the system increased. It was discovered that the thermal conductivity increased by 0.15 % vol to 12 % vol at 50°C , with the increase occurring in the range of 0.15 % vol to 12 % vol. The viscosity and density of the solution increased as the concentration of Nano particles increased, whereas these parameters reduced as the temperature increased. Increase in the concentration of nanoparticles resulted in decrease in specific heat, while increase in temperature resulted in higher specific heat. Decrease in specific heat can be attributed to lower specific heat of the Nano particles that have been introduced ([Yang et al., 2014](#)). [Joybari et al. \(2019\)](#) employed $\text{TiO}_2/\text{R134a}$ and $\text{Al}_2\text{O}_3/\text{R134a}$ nano materials having 0.06% vol with 0.1% in household refrigerator in order to decrease energy consumption and greenhouse gas emissions. The findings revealed that TiO_2 nanofluids at a concentration of 0.1% wt demonstrated the highest energy reserves, with about 25% saved. Experimental study on $\text{Al}_2\text{O}_3\text{-R134a}$ nano refrigerant in refrigeration system was conducted by [Royal et al. \(2019\)](#), and observed that the use of nano $\text{Al}_2\text{O}_3\text{-R134a}$ as refrigerant increased the COP by 3.5% and reduced the rate of power consumption while improving the compressor efficiency. Also, [Ajayi et al. \(2019\)](#) investigated the effect of Al_2O_3 nanoparticles on the working fluids of a vapour compression refrigeration system (VCRS) combined with refrigerant R134a retrofit. The system with nanorefrigerant yielded faster cooling with improved energy consumption. Moreover, ideal thermal conductivity as well as salinity was obtained, indicating that nanolubricant has better heat transfer capacity compared to base oil (Capella D).

In this paper, thermo-physical evaluation of hybrid-nanofluids zeotropic mixtures with varying different nanoparticles size of ($\text{TiO}_2/\text{Al}_2\text{O}_3/\text{CuO}$) for replacing conventional refrigerant in VCRS was conducted. The objectives were to: determine different zeotropic mixtures fraction volume concentration (contents and sizes) for HFC nanofluid refrigerant; characterize the hybrid-nanofluids zeotropic mixtures of varying different nanoparticles of ($\text{TiO}_2/\text{Al}_2\text{O}_3/\text{CuO}$); and determine the best operating mixtures for optimum performance of the VCRS. The experimental investigation revealed that global parameters in terms of thermophysical properties were altered with increase in bulk fraction, resulting in low viscosity of the hybrid nanofluids zeotropic mixtures, which facilitated easy flow of mixtures as well as improvement in the performance of VCRS when compared to conventional refrigerants. This work is restricted to evaluating the effect of varied nanofluid-zeotropic composition to determine the best optimum performance. The scope also included measurement of some global parameters along the inlet and exits axis. Areas which were not covered in this

study include leak analysis.

2. Materials and methods

A three-phase 220 V, reciprocating compressor originally designed for R12 refrigerant was used. The input power of the compressor within the system varied between 220 and 300 W. Operating parameters were obtained in two ways namely: by calculation and by measurement. Digital thermometer for temperature sensors measurement was placed on the evaporator chamber to measure the inlet and outlet temperature variations ranging from -10°C - 110°C , $\pm 3^{\circ}\text{C}$. Two inlet and outlet digital condenser pressure gauges were attached between the suction and discharge pressure for recording of the fluid flow ranging from 0.5 - 5000 Pa, $\pm 1\%$. A flow meter was also used to measure the flow rate of the refrigerant. Hitachi instrument S-3400N was used for the surface morphology study and for chemical analysis to scan the microscopy and energy dispersive X-rays analyses (EDXA). A domestic VCR test rig was used. Morphology characterization test was conducted using scanning electron microscope (SEM) and X-ray Diffraction (XRD) to determine mixture composition. For infusing and flushing out each examined sample, three service ports were created at the compressor inlet. Figure 2 illustrates the VCR test rig model. To conduct other sets of experiment, impurities and left over moisture removal was done using (ammonia) as a cleansing agent. Readings were obtained at the standard atmospheric conditions when the system is at 80% charge, and each sample investigation was done twice for accuracy.

2.1. Selecting the Proper Compressor

Knowledge of the gas, required capacity, suction pressure, suction temperature, and discharge pressure can provide a guide proper compressor selection. The basic steps according to [Akilu et al. \(2018\)](#) are as follows:

- i. Calculate the compression ratio.
- ii. Choose between a single-stage or two-stage compressor.
- iii. Calculate the discharge temperature.
- iv. Determine the volumetric efficiency.
- v. Determine the required piston displacement.
- vi. Select the compressor model.
- vii. Determine the minimum RPM required of the selected compressor.
- viii. Select an actual RPM.
- ix. Calculate the actual piston displacement.
- x. Calculate the power required.
- xi. Select appropriate options.

2.2. Operational description of the VCRES

- i. The main loop of the system under study was composed of five basic components, that is, a compressor, an evaporator, a condenser, capillary tubes and a liquid line filter-drier, as shown in Figure 1.
- ii. Hence, process 1 to 2 is compression, process 2 to 3 heat rejection in the condenser, process 3 to 4 expansion (Throttling) and process 4 to 1 is evaporation, that is, heat is absorbed by the evaporator for cooling to take place.

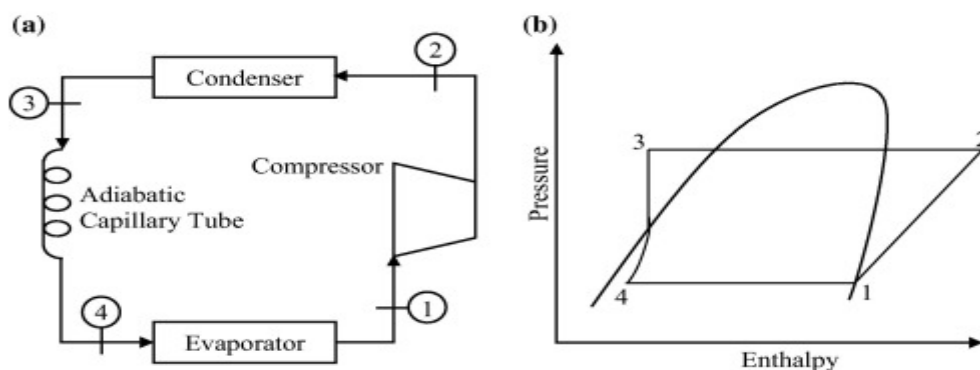


Figure 1. Thermodynamics of capillary tube refrigeration

2.3. Sample preparation/ procedure for blending nanoparticles in the based fluid

This study used an electrically drilling machine with a constructed rotating bar inserted at the drilling tip of the machine as a (magnetic stirrer or ultrasonic bath machine), which cause a stir bar immersed in the sample to form a rotating magnetic field, causing it to spin very quickly, thus stirring it. The rotating field was created by the rotating bar drilling machine, placed beneath the vessel in the mixtures. This stir bar placed within the vessel provides the stirring action in motion, driven by the electrically drilling machine. Eleven different concentration ratios were adopted and measured using digital weighing machine in bottles. A POE compressor oil of 250 ml was taken in each beaker bottles. The measured ternary particles in their % proportional ratio combination were dissolve in a standard approved POE oil sample then stirred by the probing electrical drilling machine bar for an hour to break the thermal decomposition of the solids and the formation of the precipitates into nucleation, growth, coarsening, and agglomeration, using a high shear mixing ball instrument, and a dispersion of individual or small clusters of the particles to break the attractive forces of van der Waals, thereby suspending the mixtures (with agitation). This was then followed by the dispersion of the prepared samples into the base fluid, by stirring to produce the final nanofluid. The high frequency electrically stirring provided the necessary action for the homogenization and the uniform agglomeration of the nanoparticles in the lubricant. A soluble polyolester compressor 12 oil (POE) employed as a lubricant then added to the nanoparticles by % quantity targeting to create a standard fluid mixtures. Then the required content and size of each mixture was dispersed in the base fluid after precise weighing, and subjected to stirring (blending) for an hour using kitchen blender and drilling machine. To create a uniform mixture, a digital ultrasonic device such as (kitchen blender and drilling machine) was utilized to vibrate the mixture of oil and nanoparticles for an hour, at 300 W and 15 kHz. The dispersion of the nanofluid was then monitored for an hour which no substantial sedimentation was observed. The regimented mixture of oil/nanoparticles was then injected to the zeotropic pure refrigerant. Hence, the synthesized hybridized nanolubricants of TiO_2 , Al_2O_3 , and CuO in the based fluid samples proportion (23%-R32/25%-R125/52%-R134a) prepared were kept for observation and no particle settlement was observed at the bottom of the flask containing nanofluids even after 6 hours. The same procedure was followed for the rest of the samples. Prepared samples of the nanofluid zeotropic blends are presented in Figure 2.

2.3.1. Uncertainties analysis

Preliminary tests conducted shows that high percentage volume concentration above 20% ratio will affect the pumping rate of the compressor since the mixture is thicker, thereby reducing the flow capacity of the working fluids. This will lead to the formation of agglomeration and clogging in the capillary tube, hence, generating excess heat to the compressor and condenser tubes. As a result, affecting the rate of cooling since from stages 3-4 needed a low temperature pressure gas for efficient performance. Hence, this form the bases for the choice of a suitable percentage combination mixture that will be thermally stable for efficient heat transfer coefficient. It was also notice during the uncertainties investigation that bulk volume concentration of large diameter of these materials did not allow for a larger surface of interaction with its surroundings. As calculated from the ternary graph (phase diagram grid) above, a standard percentage ratio range of 0% to 0.15% composition of the mixtures (CuO , Al_2O_3 and TiO_2) were obtained.

2.4. Experimental procedures/working

The procedures adopted for the experimental setup of the test rig is discussed under this section. A model domestic refrigerator was selected working on VCRS. Pressure and temperature gauges were installed at the inlet and outlet of the condenser component. Leakage tests were done by using soap solution. The performance of the system was investigated with the help of the measuring instrument. The mixtures (refrigerant) were charged into the system via the following process:

- i. The configuration of the drive system (compressor) was made to cater for the continuous refilling and flushing out of the working fluid mixture for ease of experimental testing which was achieved by internal valve build into the compressor.
- ii. The system was charged with the proportion of each % mass fraction mixtures
- iii. The low pressure and temperature vapour refrigerant was drawn into the compressor through the inlet or suction valve, where it is compressed to a high pressure and temperature. The high pressure and temperature vapour refrigerant was discharged into the condenser through the delivery or discharge valve.

- iv. After each successful testing and necessary result obtained, the compressor was then detached out of the system by heat process and the refrigerant flushed out per time with pressurized alcoholic based fluid (ammonia gas) as a rinsing agent to flush out any leftover of the previous fluids in the system before compressing the next refrigerant into the system.
- v. The process was repeated for all the samples.
- vi. In each testing, readings were obtained with the help of temperature and pressure gauge using the due setting time of 15 minutes.

2.5. Experimental setup

Experiment was conducted using the above procedures with hybrid nanofluids-zeotropic mixtures of (HFC-R407C) as a leading replacement for domestic refrigerators as shown in Figure 2. To record the necessary data, essential apparatus was placed at the required locations. At the exit to the evaporator and inlet to the condenser pressure gauges with $\pm 0.5\%$ accuracy was placed. A calibrated temperature sensors (thermometer) used for temperature reading. To vary the heat of the mixtures, a product of definite size and shape (water) was placed inside the evaporator chamber in order to obtain the cooling temperature and also to measure the heat of the refrigerant. The analysis was done based on the first and second law of thermodynamics and includes energy and mass balances for all components. The heat exchangers in the model were divided into individual units according to single-phase. The compression process were modelled with an isentropic efficiency of $\eta_{comp} = 0.89\%$ while losses from the compressor to the environment were disregarded. The model is implemented in Minitab 18 and uses medium properties from Microsoft Excel TM with the recommended state of the art equations of state and mixing parameters for all modelled fluid mixtures. The input power of the compressor within the system varied between 109 and 150 Watts. The evaporator is made of aluminum, submerged with a galvanized plate insulated with Styrofoam. The test rig used for this experimental study was modelled to work with R407C blended hybrid mixtures of nanoparticles, consisted of a fan cooled hermitically sealed compressor. Tests were performed after each sample enquiry to study COP, power consumption, time taken for the ambient temperature of the product to drop to its cooling time, data collected and the following performance parameters were obtained using Equation (3.10) to (3.31): refrigerating effect, evaporator heat (Q_{evap}), compressor work input (W_c), condenser heat load (Q_{cond}), Coefficient of Performance (COP), Volumetric Cooling Capacity (VCC) and pressure ratio (Pr). The experiment was conducted at the Faculty of Engineering Work shop, University of Uyo, Uyo Akwa Ibom State, Nigeria.

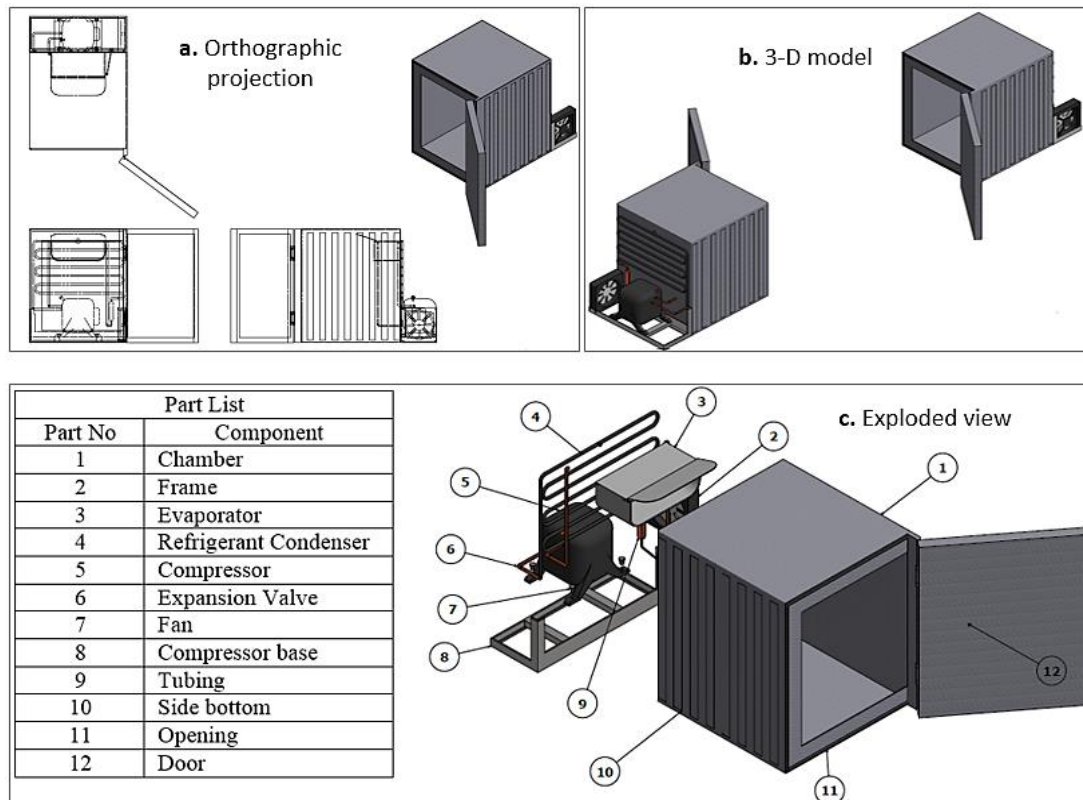


Figure 2. Vapour compression refrigeration test rig

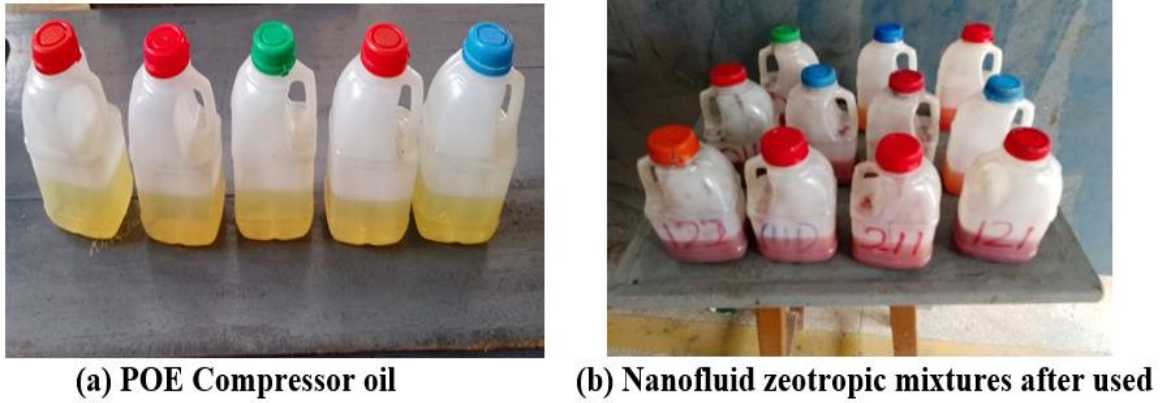


Figure 3. Sample preparation of nanofluid zeotropic blends

The following assumptions were made:

- i. Steady-state flow operation was assumed in all the system individual parts.
- ii. The working fluid has varied percentage composition throughout the cycle.
- iii. Pressure losses along each component were neglected with 75% isentropic proficiency.

Model equations for various processes of VCRS on the basis of energy and exergy were analyzed. This is considered based on bulk concentration as given by Equations 1 (Babarinde et al., 2015).

$$\omega_{no} = \frac{m_o}{(m_o+m_R)} \tag{1}$$

Bulk (volume) fraction of nanoparticle in the nanoparticle-oil suspension is given by Equation 2:

$$\psi_n = \frac{\omega_{no}\rho_o}{[\omega_{no}\rho_o+(1-\omega_{no})\rho_n]} \tag{2}$$

Where, ω = mass fraction of nano particle; ρ_r = density of pure refrigerant R407C, ρ_n = density of nano particle, m_o = mixture oil’s mass flow rate and m_R = refrigerant’s mass flow rate, M_n = mass of nano particles and M_r = mass of pure refrigerant (R407C)

Density of Hybrid-Nanofluids-Zeotropic Mixtures is derived from Equation 3:

$$P_{nf} = (1 - \phi_s)\rho_f + \phi_s\rho_p \tag{3}$$

Isobaric Specific Heat of Hybrid-Nanofluids-Zeotropic Mixtures is expressed by Equation 4:

$$C_{nf} = \frac{(1-\phi_s)P_f C_f + \phi_s \rho_p C_p}{P_{nf}} \tag{4}$$

Thermal Conductivity of Hybrid-Nanofluids-Zeotropic Mixtures is expressed as:

$$K_{nf} = kbf \left\{ \frac{[(1+2\phi)(1-(kbf/K_{TiO_2}))]/(2(kbf/K_{TiO_2})+1)}{(1-\phi(1-(kbf/K_{TiO_2}))/kbf/K_{TiO_2}+1)} \right\} \tag{5}$$

Dynamic Viscosity of Hybrid-Nanofluids-Zeotropic Mixture:

$$\mu_{nf} = \mu_{bf}(1 + 2.5\phi) \tag{6}$$

Surface tension of nanorefrigerants:

$$\sigma_{r,n,o} = \sigma_r + (\sigma_{n,o} - \sigma_r)X_{n,o}^{0.5} \tag{7}$$

The confined vapor value of refrigerant-oil combination is considered using Equation 8 (Haque et al., 2016):

$$X_{R,O} = \frac{(m_o+m_R)h_{R,O}-m_o h_o - m_R h_{R,l}}{(m_o+m_R)(h_{R,V}+h_{R,l})} \tag{8}$$

Applying Energy Balance Equation (EBE) according to Babarinde et al. (2015) is as given by Equation 9 to 14.

Work consumed by the compressor (\dot{W}_C) is given by Equation 9:

$$\dot{W}_C = \dot{m}(h_1 - h_2) \tag{9}$$

$$\text{Mass flow rate } (\dot{m}) = QE = \dot{m} \times RE \tag{10}$$

Heat rejected in the condenser (Q_c) is thus:

$$Q_c = \dot{m}(h_2 - h_3) \tag{11}$$

For capillary tube (expansion valve):

$$h_3 = \dot{m}h_4 \tag{12}$$

Heat absorbed in the evaporator (Q_e):

$$Q_e = \dot{m}(h_1 - h_4) \tag{13}$$

Coefficient of performance (COP):

$$COP = \frac{Q_e}{\dot{W}_C} \tag{14}$$

2.6. Exergy analysis of VCRS

Exergy is the maximum useful work that could be obtained from the system at a given state if the system is permitted to reach equilibrium with the environment. It predicts inefficiencies in the system and the amount of exergy destroyed within each component of the VCRS (Joybari et al., 2013). But entropy generation for a steady-flow process is expressed as:

$$S_{gen} = \sum_{out} m_e S_e - \sum_{in} m_i S_i - \sum_i \frac{Q_i}{T_i} \geq 0 \tag{15}$$

Hence, entropy generation and lost work calculated for an irreversible-adiabatic compression process can be obtained from equation 16 to 24. Considering exergy destruction in different parts of the cycle, compressor Irrevesibility was obtained using Equation 16.

$$I_{comp} = ED_{xd\ 1-2} = T_0(S_2 - S_1) \tag{16}$$

Where, $I_{comp} = ED_{xd\ 1-2}$ is the theoretical exergy damage of compressor; T_0 is the ambient temperature (K); $S_{1,2}$ is the entropy generation of working fluid at inlet and outlet of compressor (kJ/K); $I_{dest,comp}$ is exergy destruction in compressor (kW); η_m is the mechanical efficiency of the compressor. η_e is the electrical efficiency of the motor. With reference to cited literatures, it is assumed that mechanical efficiency of the compressor is 89 %.

Irreversibility or the exergy loss in the condenser is given by Equation 17.

$$I_{dest,cond} = ED_{xd\ 2-3} = q_c + T_0(S_3 - S_2) \tag{17}$$

Where, q_c is the amount of heat rejected from the refrigerant as it flows through the condenser, and can be calculated from $q_c = h_2 - h_3 = h_2 - h_3$. Irreversibility of the expansion is given by Equation 18.

$$I_{dest,exp} = ED_{xd\ 3-4} = T_0(S_4 - S_3) \tag{18}$$

The friction due to the flow of refrigerant in the evaporator and the heat transfer from the refrigerated space at a temperature of T_c are the sources for work loss, and it can be calculated using Equation 19.

$$I_{dest,evap} = ED_{xd\ 4-1} = T_0 \left((S_1 - S_4) - T_0 \left(\frac{q_{Evap}}{T_{Evap}} \right) \right) \tag{19}$$

Where, $I_{dest, evap}$ is the irrevesibility of evaporator, Q heat transfer rate in evaporator (kW); T is the temperature at exit of evaporator (K). The total exergy destruction rate (\dot{X}_{Total}) is given Equation 20. Second law Exergy Efficiency (η_{II}) is given by Equation 21.

$$\dot{X}_{Total} = (ED_{xd\ total}) = W_C + ED_{xd\ 1-2} + ED_{xd\ 2-3} + ED_{xd\ 3-4} + ED_{xd\ 4-1} \tag{20}$$

$$(\eta_{II}) = \frac{COP_{actual}}{COP_{carnot}} \tag{21}$$

One more second law parameter is exergy efficiency(η_x) given by Equation 22, which is stated as ratio of exergy of heat absorbed in evaporator to compressor work (Chaudhari & Sapali, 2017).

$$Exergeti\ Efficiency\ (\eta_x) = \frac{Carnot\ work}{Actual\ work} \tag{22}$$

Another parameter is the exergy destruction ratio (EDR) given by Equation 23, which is the ratio of total exergy destroyed in system to product’s exergy (Chaudhari & Sapali, 2017; Nayak et al., 2020).

$$EDR = \frac{1}{(\eta_x)} - 1 \tag{23}$$

2.7. Analysis of refrigerant environmental impact

The choice of refrigerant affects the lifetime warming impact of a system and the term total equivalent warming impact (TEWI) is used to describe the overall impact. It includes the effects of refrigerant leakage, refrigerant recovery losses and energy consumption. In this study, TEWI is calculated to know the actual contribution impact into the environment according to (Imre et al., 2019). The use of TEWI enables designers and contractors to estimate the equivalent CO₂ emission into the atmosphere from system leakage (direct emission) and energy consumption (indirect emission). The criteria used to estimate the total equivalent warming impact is calculated as follows:

$$TEWI = \frac{(GWP \times La \times n)}{(Direct)} + \frac{(Ea \times \beta \times n)}{(Indirect)} \tag{24}$$

Where, GWP = global warming potential, La = leakage rate (kg) per annum, n = number of years, Ea = energy consumption (kWh per annum), β = CO₂ emissions per kWh, TEWI = CO₂ (kg).

3. Results and discussion

The outcomes obtained for both measured and calculated values in the experimental study are as shown in appendix I. Figure 4 represents a plot of variation of thermal conductivity against volume fraction while Figure 5 and 6 shows the variation of density and specific heat against volume fraction. These depicted the performance characteristics of thermophysical properties between active viscosity, density, thermal conductivity, and specific heat versus varying volume concentration of the mixtures having common behavioral trend. Negligible reductions in density, specific heat, viscosities were observed for all mixtures. Like other survey, density and viscosity was establish to obtain the least charge of 0.001; whereas it has the highest optimum value of 0.002 (W/m.K) as recorded in 011 volume fraction, having zero gram-TiO₂, 7.5g-Al₂O₃/CuO. As the temperature increased, particles kinetic energy also increase, increasing the performance conductivity from 0.08 - 0.09 (W/m.K) with optimum performance recorded at (011) and 0.096 (W/m.K) having 0.075 % each of Al₂O₃ and CuO. The probable cause of this sudden increase and decrease generally not only influenced by heat of concentration, but also affected by other parameters like size and shape of each particles ratio. Moreover, the result revealed that when the operational fluid is at vapor state, thermal conductivity of nanofluid mixtures differs with temperature, but not so at liquefied state as established in the study of Henderson et al. (2015). Hence, result of this study conformed with the findings of Asadi et al. (2016), Zhelezny et al. (2017) and Maheshwary et al. (2018).

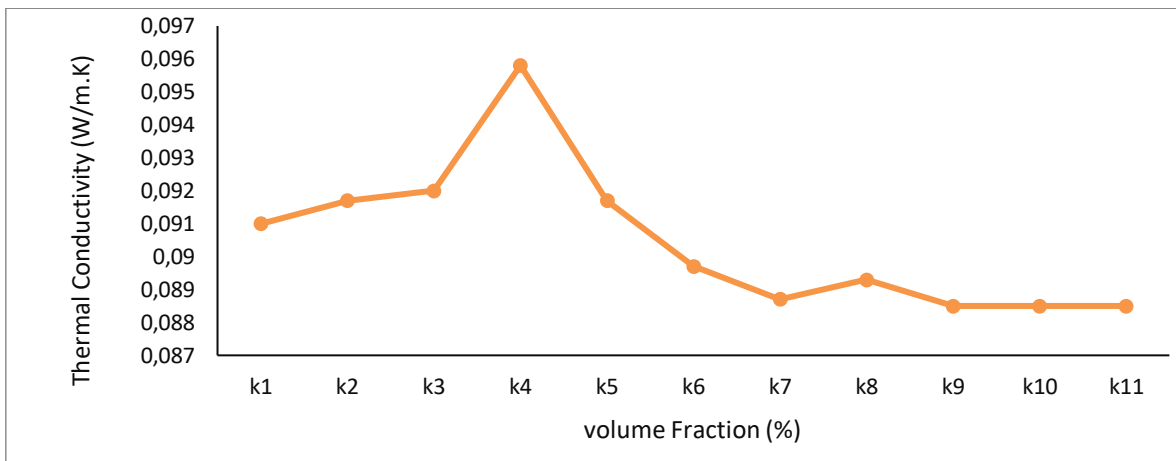


Figure 4. Plot of variation of thermal conductivity versus volume fraction

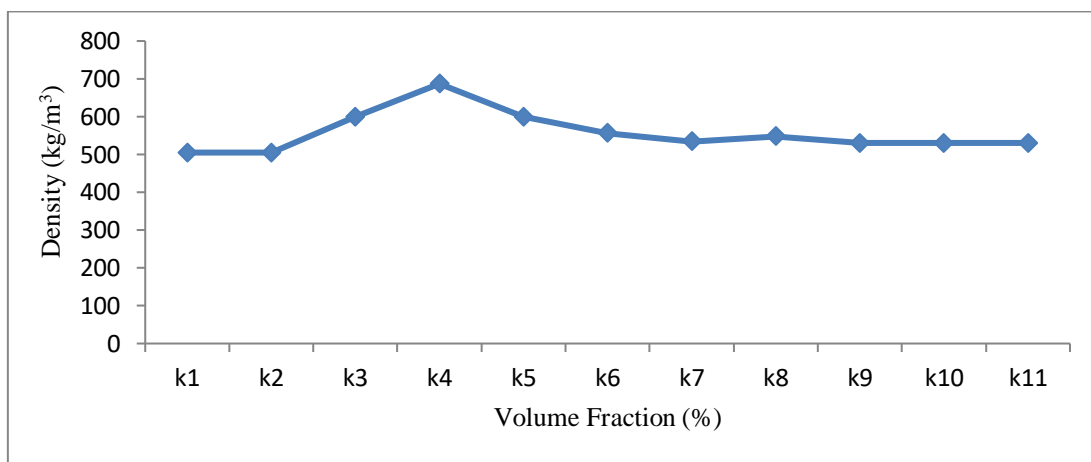


Figure 5. Plot of density versus volume fraction

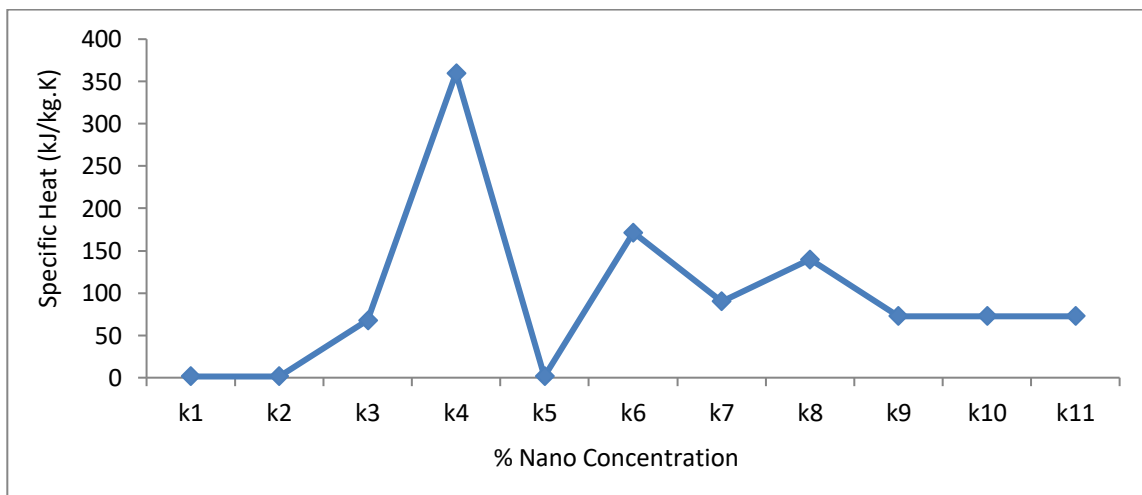


Figure 6. Plot of specific heat versus % Nano Concentration

The Coefficient of performance (COP) variation of the systems working with hybridize-nanofluids zeotropic blends (in the ratio of 011; 100; 211; 112 by weight) at different evaporator temperature is shown in Figure 5. From the Figure, it was observed that the system using hybrid combination of (011) (zero gram-TiO₂, 7.5g-

Al₂O₃/CuO blends) had the highest COP of 3.1% at refrigerant temperature of -7 °C among all examined ratios. This was followed by the system using hybrid combination of 112, 100 and 211 with COP of 1.41%, 0.69 % 0.5 % at refrigerant temperatures of -9 °C, -9 °C and -5 °C which are still adequate for the smaller compressor work requirement and higher refrigeration capacity as compared to the work done by (Babarinde et al. 2015; Nabil et al. 2017) whose COP was between 5.5% and 6.2% using LPG/R134a as well as R134a (72:28) systems respectively. The increase and sudden decrease is an indication that the compressor worked more effectively at lower particles concentration and condenser pressure, because at higher pressure, it has to deal with highly superheated refrigerant which may require more volume to be handled and correspondingly more work.

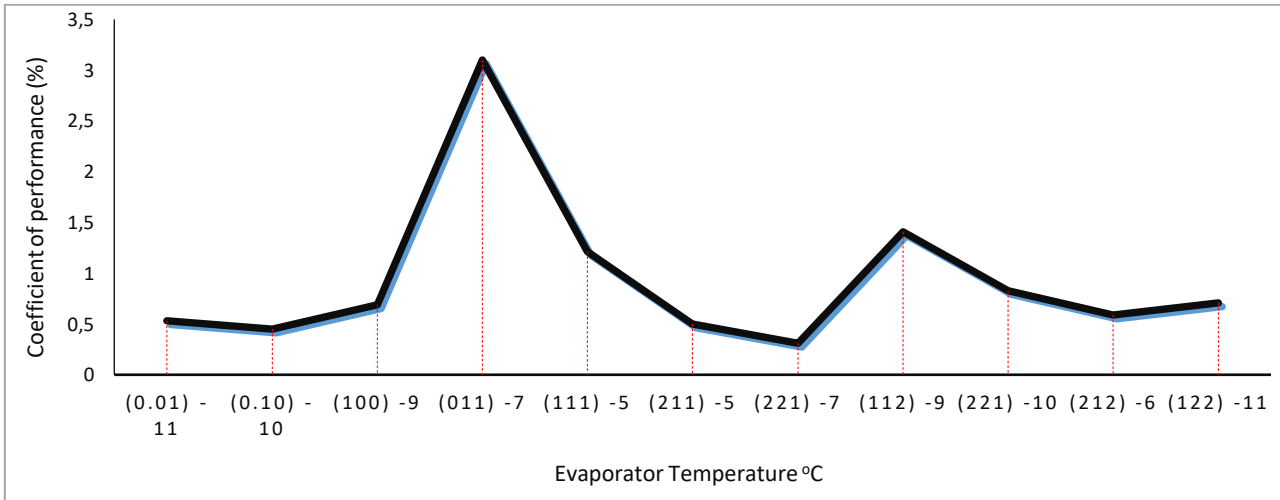


Figure 6. Plot of COP versus evaporator temperature

Compressor power requirement of a VCERS using hybridize-nanofluids zeotropic blend refrigerants are shown in Figure 6. The Figure revealed that compressor power requirement working with mixtures of (001, 100, 010) with hybrid combinations (TiO₂, Al₂O₃ and CuO) required compressor work input of 2.048, 1.229 and 1.132 at refrigerant temperatures of 11, 9 and 10 °C. The minimum compressor work input in the refrigeration system possibly takes place when there is no irreversibility which may occur as a result of friction, heat loss and other dissipative effects, as such, exergy destruction is correspondingly zero. Figure 7 represents the characterization performance of nanofluids-zeotropic mixtures, showing the morphology of mixed nanoparticles from scanning electron microscopy. This is in line with the result obtained with the work done by Akanimo et al. (2022).

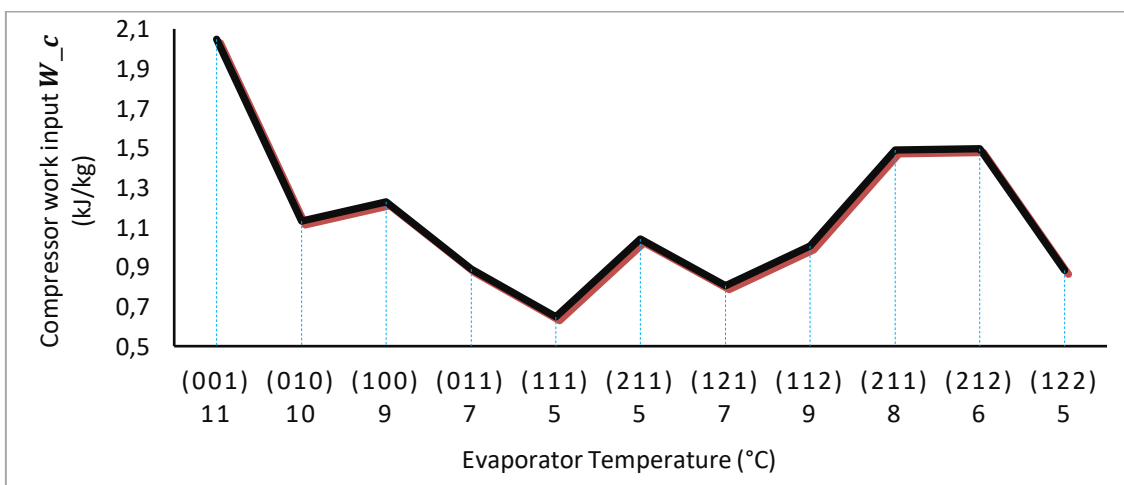
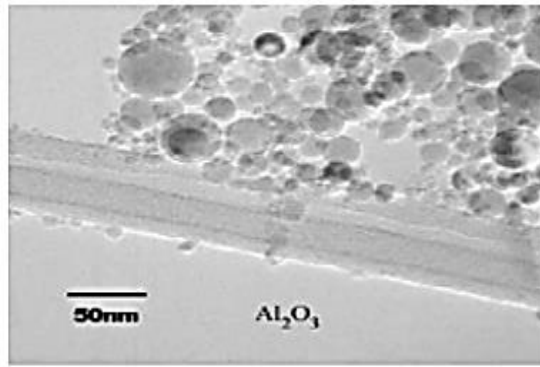
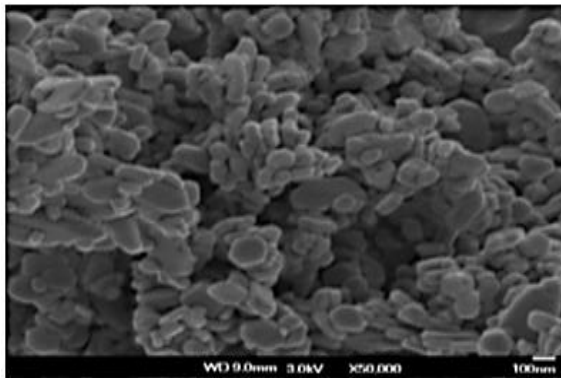


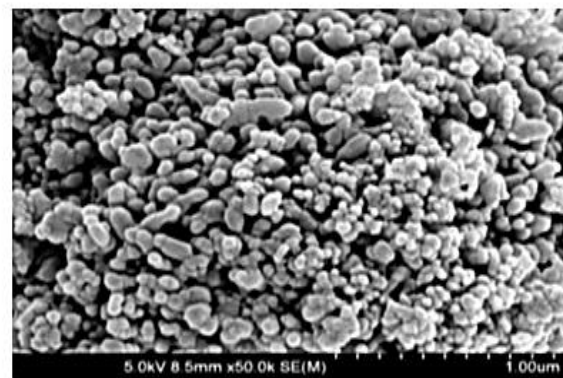
Figure 7. Plot of compressor power consumption versus evaporator temperature



(a) Aluminium Oxide Nanoparticle



(b) Copper Oxide Nanoparticle



(c) Titanium Oxide Nanoparticle

Figure 8. Images of nanoparticles obtained in a scanning electron microscope (SEM-FEG)

Graphical view of Analyzed 001 Sample of Titanium Dioxide (TiO_2) is shown in Figure 8a. Graphical view of Analyzed 010 sample of Aluminum Oxide (Al_2O_3) is shown in Figure 8b while Figure 8c represents graphical view of analyzed sample 100 of Copper Oxide (CuO).

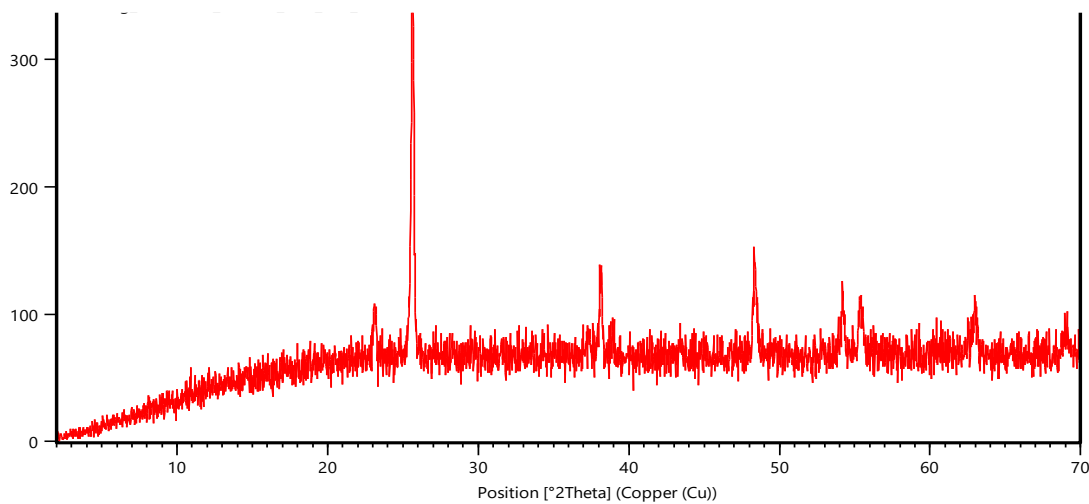


Figure 8a. Axial diffraction X-ray (XRD) spectra of titanium dioxide (TiO_2).

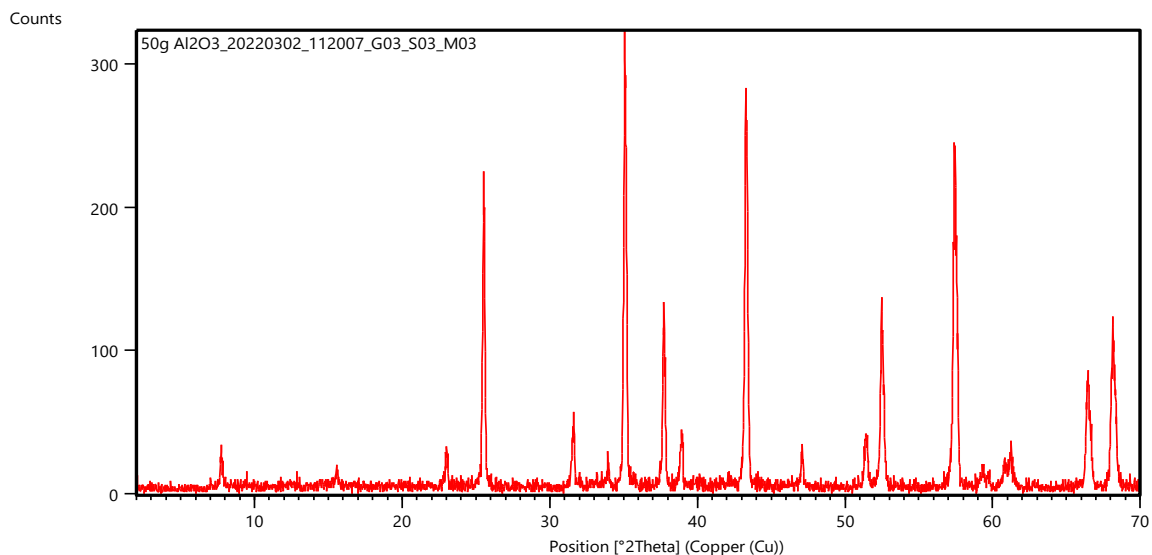


Figure 8b. Axial diffraction X-ray (XRD) spectra of aluminum oxide (Al₂O₃)

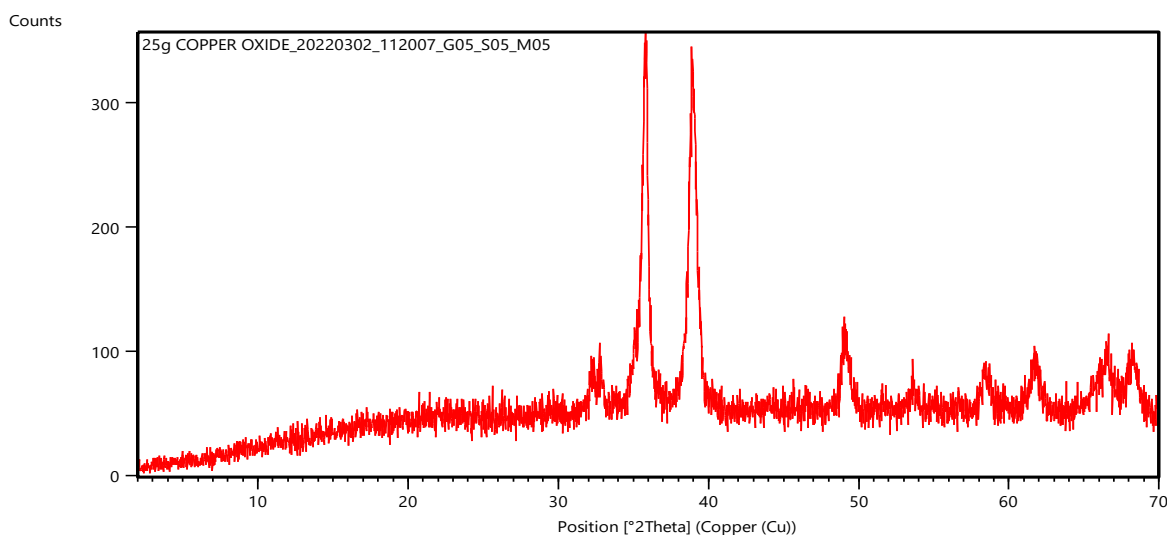


Figure 8c. Axial diffraction X-ray (XRD) spectra of copper oxide (CuO)

In this study, Hitachi instrument S-3400 N was used for the surface morphology study and chemical analysis for the microscopy was obtained from energy dispersive X-ray analyses (EDXA). The sole segment monoclinic model was established by X-ray diffraction. The micrographs demonstrated a circular and spherical combinations of aluminium oxides, titanium oxides and copper oxide nano-powders as presented in Figure 7, with particle size of less than 20 nm and 99.9%. Figure 8a revealed the pattern of TiO₂ (TONP) in XRD. Eight peaks at the angles of Bragg, at 69.0, 62.0, 55.2, 54.0, 48.0, 37.8, 25.0 and 23.0 were observed in nano α -TiO₂ (15 nm) and Debye-Scherrer expression applied to TONP crystallite size (D). The data collected corresponded to the JPDS card file No. 20220302, confirming the structure of crystallite Titania on Card Diffraction Standards (CDS). Result of XRD study using Rigaku-binary (RAW) at normal temperature of 25.00 °C, had a phase magnitude of 0.026°, with 0.154056 nm wave motion, Goniometer radius 240.00 mm, 0 kV and 0 mA. The orientation used for simulating the full width at half maximum of TiO₂ mixture was at $2\theta = 27.48^\circ$. The configuration of Al₂O₃ nanoparticles in XRD is presented in Figure 8b, with the various peak-like angles of 25.0°, 31.3°, 35.1°, 37.2°, 38.1°, 43.0°, 47.0°, 51.0°, 52.01°, 57.0°, 60.0°, 66.0° and 68.01°, suggesting that the sample were polycrystalline rooted in structure. There was no characteristic pinnacles of impurities observed, indicating the synthetization of high-quality Al₂O₃-nanoparticles (Liu et al., 2010). Also Figure 8c depicted the XRD nanoparticles of CuO. The CuO monoclinic (C2/c space party, CIPDS card No. 20220302), is possible to index all the pinnacles in CuO. High-quality nanoparticles of CuO was prepared and no peaks of impurities were observed. In XRD patterns and crystallite sizes of less than 20 nm, sharp structural peaks suggests the nanocrystalline nature of CuO nanoparticles. The topmost breadths shape of XRD mixtures of the

nanofluids were widened through accumulation of particle concentration which implied increase in the fluid eccentricity. However, the display of amorphous resulted in a better ionic diffusivity and greater ionic conductivity.

4. Conclusion

In this study, experimental performance analysis of eco-friendly alternative refrigerant in VCRS using hybrid-nanofluids zeotropic blends of varying different nanoparticles ($\text{TiO}_2/\text{Al}_2\text{O}_3/\text{CuO}$ by weight) for replacing conventional refrigerant was carried out. This was done to determine the best optimum performance blend among the selected ratios using compressor work efficiency, power consumption rate and COP as the key global parameters. The study was conducted by varying eleven different combination ratios, and results obtained served as a basis for theoretical framework. The best performance configuration of the different mixtures was determined from the experimental outcome, and the maximum measurement performance established based on three different fraction ratios between (011,112 and 111). The findings revealed that COP was found highest at (011) zero grams- TiO_2 , 7.5g- $\text{Al}_2\text{O}_3/\text{CuO}$ blend by about 3.10% and the compressor power output, volumetric cooling capacity and TEGWI were found to increase by 13.51%, 5.78% and 1.06 kg/sec CO_2 respectively. It was observed from the X-ray microscopy analysis that mixtures deposited in compressor lubricant raised the heat transfer coefficient even with a little bulk segment of 0.003% with an optimal heat transfer increase of 0.0075 Vol.% nanofluid combination. The outcome confirmed that hybrid-nanofluids zeotropic blend is an energy primary substitute, in place of conventional refrigerant in VCRS, having good environmental characteristics.

Author contribution

Akanimo Udofia: Writing, conceptualization and design; Aniekan Ikpe: Methodology, experiments, and interpretation of results. All authors contributed in their own capacity to ensure the successful completion of this research.

Declaration of ethical code

The authors declare that this research do not require any ethical committee approval or legal authorization. All authors have read and agreed to the publication of this research work.

Conflicts of interest

The authors declare that there are no conflicts of interest with the findings derived from this research work. There was no second or third party involved in the conceptualization, design, analysis, data interpretation, or decision-making on the publication of this research.

References

- Ajayi, O. O., Ukasoanya, D. E., Ogbonnaya, M., Salawu, E. Y., Okokpujie, I. P., Akinlabi, S. A., Akinlabi, E. T., & Owueyed, F. T. (2019). Investigation of the Effect of R134a/ Al_2O_3 - Nanofluid on the Performance of a Domestic Vapour Compression Refrigeration System. *Procedia Manufacturing*, 35, 112-117. <https://doi.org/10.1016/j.promfg.2019.05.012>
- Akanimo, E. U., Ikpe, A. E., & Ikpe, E. O. (2022). Exergy Performance Assessment of Hybridize-Nanofluids Zeotropic Blend as Refrigerant Replacement in Vapor Compression Refrigeration System. *III International Siirt Conference on Scientific Research*, (pp. 947-958), November 18-19, Siirt University, Turkey.
- Akilu, S., Baheta, A. T., & Sharma, K. V. (2018). Experimental measurements of thermal conductivity and viscosity of ethylene glycol-based hybrid nanofluid with TiO_2 - CuO/C inclusions. *Journal of Molecular Liquid*, 246, 396-405. <https://doi.org/10.1016/j.molliq.2017.09.017>
- Anand, S., & Tyagi, S. K. (2020). Exergy analysis and experimental study of a vapour compression refrigeration cycle. *Journal of Thermal Analysis and Calorimetry*, 110, 961-971. <https://doi.org/10.1007/s10973-011-1904-z>
- Asadi A, Asadi M, Rezaei M, Siahmargoi, M., & Asadi F. (2016). The effect of temperature and solid concentration on dynamic viscosity of MWCNT/MgO (20-80)-SAE50 hybrid nano- lubricant and proposing a new correlation: an

- experimental study. *International Communications in Heat and Mass Transfer*, 78, 48-53. <https://doi.org/10.1016/j.icheatmasstransfer.2016.08.021>
- Babarinde, T. O., Ohunakin, O. S., Adelekan, D. S., Aasa, S. A., & Oyedepo, S. O. (2015). Experimental study on LPG and R134a refrigerants in vapor compression refrigeration. *International Journal of Energy for a Clean Environment*, 16(1-4), 71-80. <http://dx.doi.org/10.1615/InterJEnerCleanEnv.2016015644>.
- Baskaran, A. K., & Mathews, P., (2015). Investigation of new eco-friendly refrigerant mixture alternative to R134a in domestic refrigerator. *Australian Journal of Basic and Applied Sciences*, 9(5), 297-306.
- Bhattad, A., Sarkar, J., & Ghosh, P. (2018). Improving the performance of refrigeration systems by using nanofluids: A comprehensive review. *Renewable and Sustainable Energy Reviews*, 82(3), 3656-3669. <http://dx.doi.org/10.1016/j.rser.2017.10.097>.
- Chaudhari, C. S., & Sapali S. N. (2017). Performance investigation of Natural Refrigerant R290 as a substitute to R22 in Refrigeration Systems. *International conference on RAAR Energy Procedia*, 109, 346-352. <https://doi.org/10.1016/j.egypro.2017.03.084>
- Flores, R. A., Aviña-Jiménez, H. M., González, E. P., & González-Uribe, L. A. (2019). Aerothermodynamic design of 10 kW radial inflow turbine for an organic flashing cycle using low-enthalpy resources. *Journal of Cleaner Production*, 251, 119713. <http://doi.org/10.1016/j.jclepro.2019.119713>
- Haque, M. E., Bakar, R. A., Kadrigama, K., Noor, M. M., & Shakaib, M. (2016). Performance of a domestic refrigerator using nanoparticles-based polyolester oil lubricant. *Journal of Mechanical Engineering and Sciences*, 10(1), 1778-1791. <http://dx.doi.org/10.15282/jmes.10.1.2016.3.0171>
- Haque, M. E., Bakar, R. A., Kadrigama, K., Noor, M. M., & Shakaib, M. (2016). Performance of a domestic refrigerator using nanoparticles-based Polyolester oil lubricant. *Journal of Mechanical Engineering and Sciences*, 10(1), 1778-1791. <https://doi.org/10.15282/jmes.10.1.2016.3.0171>
- Henderson, K., Park, Y., Liu, L., & Jacobi, A. M. (2010). Flow boiling heat transfer of R134a-based nanofluids in a horizontal tube. *International Journal of Heat and Mass Transfer*, 53(5-6), 944-951. <https://doi.org/10.1016/j.ijheatmasstransfer.2009.11.026>
- Imre, A., Kustán, R., & Groniewsky, A. (2019). Thermodynamic selection of the optimal Working fluid for organic Rankine cycles. *Energies*, 12(10), 20-28. <https://doi.org/10.3390/en12102028>
- Joybari, M. M., Hatamipour, M. S., Rahimi, A., & Modarres, F. G. (2013). Exergy analysis and optimization of R600a as a replacement of R134a in a domestic refrigerator system. *International Journal of Refrigeration*, 36(4), 1233-1242. <https://doi.org/10.1016/j.ijrefrig.2013.02.012>
- Joybari, M. M., Seddegh, S., Wang, X., & Haghghat, F. (2019). Experimental investigation of multiple tube heat transfer enhancement in a vertical cylindrical latent heat thermal energy storage system. *Renewable Energy*, 140, 234-244. <http://doi.org/10.1016/j.renene.2019.03.037>
- König-Haagen, A., Höhlein, S., & Brüggemann, D. (2020). Detailed exergetic analysis of a packed bed thermal energy storage unit in combination with an Organic Rankine Cycle. *Applied Thermal Engineering*, 165, 114583. <https://doi.org/10.1016/j.applthermaleng.2019.114583>
- Krauzina, M. T., Bozhko, A. A., Krauzin, P. V., & Suslov, S. A. (2017). Complex behavior of a nanofluid near thermal convection onset: Its nature and features. *International Journal of Heat and Mass Transfer*, 104, 688-692. <https://doi.org/10.1016/j.ijheatmasstransfer.2016.08.106>
- Krishna, S., Gobinath, N., Sajith, N. V., Sumitesh, D., & Sobhan, C. B. (2012). Application of TiO₂ nanoparticles as a lubricant-additive for vapour compression refrigeration systems: An experimental investigation. *International Journal of Refrigeration*, 35(7), 243-283. <https://doi.org/10.1016/j.ijrefrig.2012.07.002>
- Liu, Z. H., & Zhu, Q. Z. (2011). Application of aqueous Nanofluids in a horizontal mesh heat pipe. *Energy Conversion and Management*, 52(1), 292-300. <https://doi.org/10.1016/j.enconman.2010.07.001>
- Maheshwary, P. B., Handa, C. C., & Nemade, K. R. (2018). Effect of Shape on Thermophysical and Heat Transfer Properties of ZnO/R-134a Nanorefrigerant. *Materials Today: Proceedings*, 5(1), 1635-1639. <https://doi.org/10.1016/j.matpr.2017.11.257>

- Nabil, M. F., Azmi, W. H., Hamid, K. A., Zawawi, N., Priyandoko, G., & Mamat, R. (2017). Thermophysical properties of hybrid nanofluids and hybrid nanolubricants: A comprehensive review on performance. *International Communications in Heat and Mass Transfer*, 83, 30-39. <https://doi.org/10.1016/j.icheatmasstransfer.2017.03.008>
- Nayak, A. K., Hagishima, A., & Tanimoto, J. (2020). A simplified numerical model for evaporative cooling by water spray over roof surfaces. *Applied Thermal Engineering*, 165, 114514. <https://doi.org/10.1016/j.applthermaleng.2019.114514>
- Paula de, C. H., Duarte, W. M., Rocha T. T. M., Oliveria R. N., & Maia A. A. T. (2020). Optimal Design and Environmental, Energy and Exergy Analysis of a VCR System using R290, R1234yf, and R744 as Alternatives to replace R134a. *International Journal of Refrigeration*, 113, 10-20. <http://dx.doi.org/10.1016/j.ijrefrig.2020.01.012>
- Rasti, M., Aghamiri, S., & Hatamipour, M. S. (2013). Energy efficiency enhancement of a domestic refrigerator using R436A and R600a as alternative refrigerants to R134a. *International Journal of Thermal Sciences*, 74, 86-94. <https://doi.org/10.1016/j.ijthermalsci.2013.07.009>
- Royal, M. V., Ahamed, M., Kumar, R., & Krishna, H. (2019). Experimental Study on Al₂O₃-R134a Nano Refrigerant in Refrigeration System. *Journal of Emerging Technologies and Innovative Research*, 6(5), 161-166.
- Sabareesh, R. K., Gobinath, N., Sajith, V., Das, S., & Sobhan, C. B. (2012). Application of TiO₂ nanoparticles as a lubricant-additive for vapor compression refrigeration systems-An experimental investigation. *International journal of refrigeration*, 35(7), 1989-1996. <https://doi.org/10.1016/j.ijrefrig.2012.07.002>
- Sarkar, J., Bhattacharya, S., Lal, A. (2013). Selection of suitable natural refrigerants pairs for cascade refrigeration system. *Proceedings of the Institution of Mechanical Engineers Part A: Journal of Power and Energy*, 227(5), 612-622. <https://doi.org/10.1177/0957650913487730>
- Selvam, C., Lal, D. M., & Harish, S. (2016). Thermophysical properties of ethylene glycol-water mixture containing silver. *International Journal of Research in Engineering and Innovation*, 30, 1271-1279. <https://doi.org/10.1007/s12206-016-0231-5>
- Yang, Z., Liu, B., & Zhao, H. (2004). Experimental study of the inert effect of R134a and R227ea on explosion limits of the flammable refrigerants. *Experimental Thermal and Fluid Science*, 28(6), 557-563. <https://doi.org/10.1016/j.expthermflusci.2003.06.005>
- Zhang, X., Wang, F., Fan, X., Duan, H., & Zhu, F. (2017). An investigation of a heat pump system using CO₂/propane mixture as a working fluid. *International Journal of Green Energy*, 14(1), 105-111. <https://doi.org/10.1080/15435075.2016.1253577>
- Zhelezny, V. P., Lukianov, N. N., Khliyeva, O. Y., Nikulina, A. S., & Melnyk, A. V. (2017). A complex investigation of the nanofluids R600a-mineral oil-Al₂O₃ and R600a-mineral oil-TiO₂. Thermophysical properties. *International Journal of Refrigeration*, 74, 488-504. <https://doi.org/10.1016/j.ijrefrig.2016.11.008>

Appendices

Appendix 1. Calculated values of exergy destruction in each component at various % fractions

Particles Conc (%)	Compressor (kW)	Condenser (kW)	Expansion valve (kW)	Evaporator (kW)	Total Exergy Destruction	Mean Cooling Time (S)	R_E	W_c (kJ/kg)	$\eta_{\text{exergetic}}$ (%)	\dot{m} (kg/s)	COP	Power consumption (kW)
(001)	3.283	68.46	44.41	-2.415	111.54	19.5	3.1	2.048	0.54	0.225	0.53	2.199
(010)	1.062	45.77	40.62	-0.651	86.71	18	2.3	1.132	0.76	0.222	0.45	1.216
(100)	1.394	47.96	42.66	-1.129	90.89	12.5	3.6	1.229	0.73	0.236	0.69	1.319
(011)	41.99	48.48	44.72	-9.369	125.82	14	12.1	0.888	1.43	0.225	3.10	0.942
(111)	1.332	46.15	40.76	-1.059	39.73	18	3.5	0.648	0.32	0.224	1.21	0.696
(211)	1.071	51.67	45.31	-0.663	97.39	20	2.3	1.040	0.94	0.226	0.50	1.117
(121)	0.671	41.43	36.83	0.248	78.57	17	1.2	0.806	0.97	0.207	0.31	0.866
(112)	0.839	48.85	43.87	0.937	94.41	15.5	6.5	1.006	0.93	0.219	1.41	1.081
(221)	1.395	40.32	43.98	0.964	84.11	15.5	5.7	1.488	0.57	0.216	0.83	1.598
(212)	1.454	39.63	43.86	1.266	82.71	14.5	8.7	1.497	0.55	0.214	0.59	1.608
(122)	1.550	45.31	41.86	1.525	90.25	14	3.0	0.881	1.02	0.210	0.71	0.955

Nomenclature

A	Surface area of Tubes
C	Specific Heat
CFCs	Chloro fluorocarbon
COP	Coefficient of Performance
EDXA	Energy Dispersive X-rays Analyses
h	Specific Enthalpy
HCFC	Hydrochlorofluorocarbon
HFC	Hydrofluorocarbon
PR	pressure Ratio
Q	Heat Transfer Rate
SEM	Scanning Electron Microscope
T	Temperature
U	Overall heat transfer coefficient
VCC	Volumetric Cooling Capacity
W	Power consumption of compressor
XRD	X-ray Diffraction
TEWI	Total equivalent warming impact
T_0	Ambient temperature (K)
ρ_{bf}	Bulk fluid density
ρ_{nf}	Density of nanofluids (kg/m ³)
ρ_r	Density of pure refrigerant
$S_{1,2}$	Entropy generation of working fluid at inlet and outlet of compressor (kJ/K)
$I_{dest,comp}$	Exergy destruction in compressor (kW)
K_{TiO_2}	Thermal conductivity of TiO ₂ nanoparticle equal (11.8 W/m.K).
K_{bf}	Thermal conductivity of base fluid at 25 °C (0.08779 W/m.K),
\emptyset	Volume fraction
m_o	Mixture oil's mass flow rate
M_n	Mass of nano particles
\dot{m}_r	Mass flow rate
ω	Mass fraction of nano particle
ϕ_s	Nanoparticles percentage (%)
C_{nf}	Specific heat of nanofluids (J/kg K)
C_p	Specific heat of nanoparticles (J/kg K)
I_{comp}	Theoretical exergy damage of compressor